Usefulness of 99mTc-pertechnetate SPECT-CT in thyroid tissue volumetry: phantom studies and a clinical case series

Usefulness of 99mTc–pertechnetate SPECT-CT in thyroid tissue volumetry: phantom studies and a clinical case series

Enrico Calandri[a], MD, Maria Teresa Giraudo[b], PhD, Roberta Sirovich[b], PhD, Antonella Ostan[c], MPE, Mirco Pultrone[a], MD, (altri[d] ……), Lucia Conversano[a], MD, Paolo Bagnasacco[e], MD, Sonya Gallina[a], BSc, Giuseppe De Vincentis[d], MD, PhD.

- **a Department of Medicine and Urgency, Nuclear Medicine Unit, Ospedale degli Infermi, Ponderano (BI), Italy.**
- **b Department of Mathematics G. Peano, University of Torino, Torino, Italy.**
- **c Health Physics Department, Azienda Ospedaliera Maggiore della Carità, Novara, Italy.**
- **d Department of Radiological Sciences, Oncology and Anatomical Pathology, Nuclear Medicine Unit, "Sapienza" University, Rome, Italy.**
- **e Department of Medicine and Urgency, Radiotherapy Unit, Ospedale degli Infermi, Ponderano (BI), Italy.**

Key Words: thyroid, hyperthyroidism, thyroid tissue volumetry, SPECT, SPECT-CT.

ABSTRACT

Background: An accurate measurement of the target volume is of primary importance in theragnostics of hyperthyroidism. **Objective:** Our purpose was to evaluate the accuracy of a threshold–based isocontour extraction procedure for thyroid tissue volumetry from SPECT-CT. **Methods:** Cylindrical vials with a fix volume of $^{99m}TcO_4$ at different activities were inserted into a neck phantom in two different thickness settings. Images were acquired by orienting the phantom in different positions, i.e. 40 planar images and 40 SPECT-CT. The fixed values of the iso-contouring threshold for SPECT and SPECT-CT were calculated by means of linear and spline regression models. Mean, Median, Standard Deviation, Standard Error, Mean Absolute Percentage Error and Root Mean-Square Error were computed. Any difference between planar method, SPECT and SPECT-CT and the effective volume was evaluated by means of ANOVA and post-hoc tests. Moreover, planar and SPECT-CT acquisitions were performed in 8 patients with hyperthyrodism, considering relevant percentage differences greater than > 20 % from CT gold standard.

Results: Concerning phantom studies, the planar method show higher values of each parameters than the other two methods. SPECT-CT shows lower variability. However, no significant differences were observed between SPECT and SPECT-CT measurements. In patients, relevant differences were

found in 7 out of 9 lesions with planar method, in 6 lesions with SPECT, but in only one with SPECT-CT.

Conclusion: Our study confirms the superiority of SPECT in volume measurement if compared with the planar method. A more accurate measurement can be obtained from SPECT-CT.

(max 250 parole)

1. INTRODUCTION

High accuracy in the measurement of the target volume plays an important role in the successful outcome in radioiodine treatment of hyperthyroidism. High-resolution Ultrasound (US) is considered the best imaging technique for evaluating the thyroid gland, but is limited by intraobserver and interobserver variability in the measurements [1, 2]. However, a greater accuracy in volume estimation has been demonstrated when a three-dimensional US is available, with low intraobserver variability and high repeatability [3]. US has, in any case, a well-known limit in accessibility to the retrosternal portion of a goiter [4]. Other methods are Computed Tomography (CT) and Magnetic Resonance (MR), although poorly used for this purpose for there high costs and scarce availability. Moreover, the volume measured with all these techniques does not always reflect the target volume of radioiodine therapy, that is only the hyperfunctioning one.

Different methods, based on the correlation between the cross-sectional gland area in the frontal scintigraphic image and the volume, have been previously developed for estimating the thyroid mass [5].These methods are based on a certain geometric assumption regarding the configuration of the thyroid. Therefore, they present an intrinsic bias given by the assumption of the equivalence between the measured axes and those of a rotation ellipsoid, resulting in a possible underestimate or overestimate of the mass [5, 6]. Sometimes the hyperfunctioning tissue cannot be a priori assimilated to a rotation ellipsoid, for example in presence of a group of contiguos hot nodules or in case of drastically enlarged or abnormally shaped basedowied goiters. We described a large hyperfunctioning residue of the thyroglossal duct not attributable to a regular geometric shape at Single Photon Emission Computed Tomography - Computed Tomography (SPECT-CT) images [7].

Since the 90s, Single Photon Emission Computed Tomography (SPECT) has proven to be more accurate in the estimation of the thyroid volume than planar scintigraphy, even without attenuation and scatter correction [5, 8, 9]. Scientific data, obtained from the application of SPECT-CT in benign thyroid pathology, are instead limited, especially in a modern approach to radioiodine treatment of hyperthyroidism, through the combined use of diagnostics and therapy, currently known as “theranostics” or, better, “theragnostics” [10]. To our knowledge, no fix threshold-based volumetry method from 99mTc–pertechnetate SPECT-CT in benign thyroid disorders has been reported so far.

Therefore, the aim of this study was to evaluate the accuracy of a threshold –based isocontour extraction procedure for thyroid tissue volumetry from hybrid SPECT-CT technology. For this purpose, we evaluated through phantom studies three different methods, obtained from planar scntigraphy, SPECT and SPECT-CT respectively. Furthermore, the measurements obtained with the three methods in patients affected by hot nodules, Graves' disease and a hyperfunctioning ectopic tissue are reported here, considering CT as a gold standard. Both in phantom studies and in a clinical case series, we investigated the measurement accuracy with particular regard to the depth of the radioactive volume.

2. MATERIALS AND METHODS

2.1 Phantom studies

Five cylindrical vials were obtained for planar images at activities of 2.9 MBq, 6.2 MBq, 8.7 MBq, 11.86 MBq, 14.74 MBq and five ones were also obtained for SPECT-CT at activities of 2.98 MBq, 6 MBq, 8.61 MBq, 11.92 MBq, 14.82 MBq, each in a volume of 15 ml of $^{99m}TcO_4^-$ solution. Each vial was inserted into a neck phantom of poly(methyl methacrylate) (PMMA) (Biodex Medical System) in two different anterior thickness settings: "p" (minimum thickness) and "g" (maximum thickness), obtained by rotating the carrier inside the phantom's cylinder (**Figure 1**). Planar and SPECT-CT images were acquired by orienting the neck phantom in different positions: 00.00 in which the phantom is in horizontal position along the axis of the bed; 00.25 in which it is inclined by 25° on the sagittal plane, 25.00 in which the phantom, in horizontal position, is inclined by 25° laterally; 25.25 in which it is oriented by 25° both with respect to both coronal and sagittal plane (**Figure 2**). In all cases we took 8 planar and 8 SPECT-CT acquisitions (p 00.00, g 00.00, p 00.25, g 00.25, p 25.00, g 25.00, p 25.25, g 25.25) for each vial of different activity, i.e. 40 planar images and 40 SPECT-CT. These different acquisition modalities for each vial reflect the possibility of having patients with both thin and fat necks, and patients who, for various reasons, cannot be acquired with an ideal neck orientation. Moreover, all acquisitions can be divided into two groups, A and B, according to the shape taken by the radioactive liquid inside each vial with respect to the orientation of the neck phantom. Acquisitions p 00.00, g 00.00, p 25.00, g 25.00 were included in group A and acquisitions p 00.25, g 00.25, p 25.25, g 25.25 were included in group B (**Figure 3**).

Planar scans and SPECT-CT were performed using a dual head γ-camera with an integrated 16 slices CT for combined transmission and emission tomography (GE Discovery 670 Pro), equipped with low energy high resolution collimators set in H-mode. The study protocol consisted in a 5 minutes of acquisition, in a 128 x 128 matrix, at a distance of 10 cm in anterior view for planar images, and in

60 projections in a 128 x 128 matrix, at 15 s for view, a zoom factor of 1.0, automated body contour detection for SPECT; CT acquisitions were performed at 120 keV, 60 mA and a slice thickness of 2.5 mm.

Therefore, three measurement systems called planar method, SPECT method and SPECT-CT method were carried out:

2.2 Planar method

A 9-point smoothing filter was applied to the planar image of the mediastinum without electronic magnification. According to the protocol in use in our Department, an iso-contouring ROI with a threshold of 40% was drawn and, subsequently, an elliptical ROI drawn manually was superimposed. The short and long axes were measured for each ellipse and the target volume was then estimated according to the following formula of the rotation ellipsoid: $V = \pi / 6 \times a \times b^2$, where V is the volume, a and b are the major and the minor axes [11].

2.3 SPECT and SPECT-CT method

Each SPECT-CT acquisition has been processed on GE Xeleris Workstation (version 3.1) using Volumetrix Evolution software. Two iterative reconstructions (OSEM, 2 iterations, 10 subsets) were obtained, differing in the use of the attenuation correction by means of CT and of an algorithm of resolution recovery (Volumetrix Evolution) in each other. No scatter correction has been applied. They are respectively named IRACRR (iterative reconstruction CT-based attenuation correction resolution recovery) and IRNC (iterative reconstruction no attenuation correction). In each axial series, the three threshold of isocontour ROIs which best allowed to estimate the volume from the sum of all slices were found. The fixed values of the threshold for both methods (SPECT: 50 %, SPECT-CT: 41 %) were then calculated by means of linear and spline regression models for the dependency of the volume estimation error on the chosen threshold [12]. The optimal values were found by minimizing the error by identifying the intersection of the fitted error with the horizontal axes in the linear model and the flattening point in the spline model (**Figure 4**) The linear and spline regression methods gave very similar results and the fixed threshold values were used to recalculate the volumes (**Figure 5**).

2.4 Statistical analysis

Statistical analysis was performed using R software version 4.0.3. The Mean, the Median, the Standard Deviation (SD), the Standard Error (SE), the Mean Absolute Percentage Error (MAPE) and the Root Mean-Square Error (RMSE) were computed for each method. Any difference in volume

calculation from phantom studies between planar method, SPECT and SPECT-CT and the effective volume was evaluated by means of ANOVA and post-hoc tests, and p-values are reported. Where feasible, confidence intervals for measurement error were also computed.

2.5 Patient studies

From July 2019 to February 2021 a SPECT-CT protocol was performed in a total of 14 patients affected by hyperthyroidism. The hybrid image study was considered a useful tool for a better definition of the relationships with the adjacent anatomical structures, in addition to thyroid planar scintigraphy. Each patient received a fixed dose of 148 MBq of 99mTc-pertechnetate ($^{99m}TcO_4^-$). After 15 minutes, a thyroid image (zoom factor of 2), a mediastinal image and a SPECT-CT with the same acquisition parameters as the phantom studies mentioned above were acquired respectively. Four patients were excluded from the study because the target volume was not optimally delineable in CT images (2 patients) or in SPECT and in SPECT-CT reconstructions (2 patients). Two patients were excluded due to the greater activity of the salivary glands compared to the thyroid tissue, not allowing the correct use of iso-contouring ROIs. Therefore only 8 patients (average age 59 years, age range 29-78 years, 5 male and 3 female) were considered eligible for the study. Four patients had solitary hot nodule and 4 Graves' Disease. One of the latter had also an ectopic tissue developing caudally from the hyoid region and clearly separated from the thyroid lobes. Each potential target volume was estimated by planar, SPECT and SPECT-CT method, with CT as the reference. Only one expert clinician for each procedure, planar (L. C.), SPECT (E. C.), SPECT-CT (M. P.) and CT (P. B.) respectively, performed all the elaborations. In the patient with basedowefied ectopic tissue, the calculation was performed on coronal slices to avoid that the iso-contouring ROIs included hyperfunctioning thyroid tissue. In all other cases the ROIs were drawn on the axial slices.

The CT images, acquired for attenuation correction, were transferred to Treatment Planning System RayStation 8A (RaySearch Laboratories) to make the volumetric analysis of the ROIs. On each axial slice of CT a contouring ROI of the structure under examination was created using the tools provided by the software. The system then allowed to view the volumetric result of what was contoured, allowing any changes to be made to the contours, also in coronal and sagittal sections. Finally, the volume of each designed structure was calculated automatically by the software (**Figure 6**).

3. RESULTS

Figure 7 and **Figure 8** show the boxplots and histograms of the error measurements in phantom studies, for the three methods. **Table 1** shows the corresponding values of the Mean, the Median, the SD, the SE, the MAPE and the RMSE.

	PLANAR	SPECT	SPECT-CT
Mean [ml]	0.4729	0.0703	-0.2340
Median [ml]	0.433	0.023	-0.3225
SD [ml]	1.8033	1.1917	1.0618
MAPE [%]	10.3988	6.1867	6.0775
SE [%]	1.9009	1.2562	1.1192
RMSE [ml]	1.8423	1.1788	1.0743

Table 1: Mean, Median, SD, MAPE, SE and RMSE of measurement errors for the three methods planar, SPECT and SPECT-CT.

Regarding the planar method, all parameters show higher values than the other two methods. SPECT-CT shows lower variability; in fact, SD, SE and RMSE show the lowest values. Moreover, the MAPE is minimized by SPECT-CT method. Based on our results, although it is not possible to exclude that SPECT-CT underestimates the volume measurements (p-value = 0.0856 for alternative hypothesis mean less than zero), no significant differences were observed between SPECT and SPECT-CT measurements and weak significance was obtained between planar and SPECT-CT. Statistical significance was calculated through ANOVA (p-value = 0.0784) and post-hoc t.test with Bonferroni correction (planar-SPECT and SPECT-SPECT-CT pvalue > 0.5, planar-SPECT-CT pvalue = 0.0744). The planar method showed significantly higher values than the gold standard (95% confidence interval for the measurement error = (-0.1038, 1.0496) and p-value = 0.0526 of the t-test for the mean measurement error greater than 0).

Table 2 shows the values of Mean, Median, SD, SE, MAPE and RMSE for the different depths, p and g. Regarding the SPECT-CT method, it is interesting to note that this subanalysis shows lower SD, SE, MAPE and RMSE values for depth p than for depth g.

	SPECT		SPECT-CT	
	p	g	p	g
Mean [ml]	0.053	0.0876	-0.1931	-0.275
Median [ml]	-0.02	0.066	-0.193	-0.3655
SD [ml]	1.2573	1.1548	1.0222	1.1251
MAPE [%]	6.5453	5.8280	5.7683	6.3867
SE [%]	1.8743	1.7214	1.5238	1.6771
RMSE [ml]	1.2266	1.1289	1.0149	1.1305

Table 2: Mean, Median, SD, MAPE, SE and RMSE for the two methods SPECT and SPECT-CT and for the two depths p and g.

The volumes measured by means of the three different methods in patient studies are displayed in **Table 3**. We considered as relevant percentage differences greater than > 20 % from the measurements obtained with CT. We found relevant differences in 7 out of 9 lesions with planar method and in 6 out of 9 with SPECT method, but in only 1 out of 9 lesions with the SPECT-CT method. Moreover, SPECT-CT provided more accurate measurements than the other two methods in 7 out of 9 lesions.

Patients	Lesion	Target Volume	Planar (ml)	% diff.	SPECT (ml)	% diff.	SPECT-CT (ml)	% diff.	CT (ml)
	a	ectopic tissue	6.4	-8.05	9.4	35.06	7.16	2.87	6.96
1	b	Graves' Disease	10.14	-47.16	14.66	-23.61	21.06	9.74	19.19
2	c	retrosternal hot nodule	29.01	-32.16	34.09	-20.28	40.91	-4.33	42.76
3	d	retrosternal hot nodule	17.87	11.55	10.35	-35.39	16.66	4.00	16.02
4	e	hot nodule	4.57	31.70	4.83	39.19	5.52	59.08	3.47
5	f	hot nodule	18.32	-28.83	22.27	-13.48	22.01	-14.49	25.74
6	g	Graves' Disease	42.59	-30.04	52.22	-14.22	53.43	-12.24	60.88
7	h	Graves' Disease	23.11	-27.92	34.35	7.14	34.18	6.61	32.06
8	i	Graves' Disease	17.37	-52.29	27.88	-23.43	30.55	-16.09	36.41

Table 3: Volume measurements in milliliters and percentage difference from the gold standard value obtained by CT for each of the three methods under comparison (planar, SPECT and SPECT-CT).

4. DISCUSSION

Thyroid scintigraphy is a high sensitive and specific functional imaging, able to investigate every altered functional state of thyroid conditioning autonomy. It is generally performed with $^{99m}TcO_4^-$ produced by a $^{99}Mo/^{99}Tc$-generator. After intravenous injection, $^{99m}TcO_4^-$ shows a loose bound to plasma proteins and moves rapidly out of the intravascular compartment. Na^+/I^- symporter allows its carriage into the follicular thyroid cell without organification in the gland. The Thyroid Uptake of $^{99m}TcO_4^-$ (TCTU) shows a plateau phase between 15' and 30' minutes. In the geographic areas with sufficient iodine supply the absolute uptake of $^{99m}TcO_4^-$ ranges from 0.3% and 3% of the administered activity, whereas the range extends from 1.2% to 7% in iodine deficiency areas [13]. TCTU is calculated according to the following formula: TCTU(%) = (counts over thyroid – background counts x)100 / counts of injected activity [14]. Without TSH suppression, TCTU has a limited clinical value. Factors influencing his determination are mainly thyroid volume, iodine supply and patient's age. A

substantial overlap of TCTU values can be observed between endemic goiter, euthyroid, thyreotoxic autonomy and Graves' disease Extreme values are specific respectively for Graves' disease (TCTU > 15%) and iodine contamination (TCTU < 0.3%) [13, 14].

According to the data mentioned above, each vial was filled with a $^{99m}TcO_4^-$ solution in 15 ml of volume, at activity equal to 2%, 4%, 6%, 8% and 10% of 148 MBq, that generally administered for thyroid scintigraphy in adult patients in our Nuclear Medicine Unit. Therefore, a first limit is given by the activity tested in the phantoms, with a range from 0.19 MBq/ml to 0.99 MBq/ml for SPECT and SPECT-CT studies and 0.19 MBq/ml to 0.98 MBq/ml for planar studies.

Regarding the choice of a fix volume, it is worth mentioning that there is no unanimous consensus in literature on the normal size of the thyroid in adults, obtained by ultrasonography (1). Rumack et al. found an adult normal value of 10-11 ± 3 ml [15]. For Nataf et al. the normal values are > 18 ml for women and > 20 ml for men [16]. Riccabona found normal values below 18 ml in adult males and below 25 ml in adult females, but limited to the Austrian population [17]. We have decided to use a fixed volume of 15 ml which, according to the orientation of the liquid in the vial, takes on two different irregular shapes, both akin to a hypertrophic thyroid lobe or to a nodular conglomerate. Nevertheless, it represents another limit to the present study, in relation to the different impact of the partial volume effect in phantoms of different sizes reported in previous studies, generally consisting of rotation ellipsoids or spheres. Developing a tissue-specific dosimetry method based on planar images, Matheoud et al. introduced in a thyroid phantom three spheres containing ^{123}I in solution, respectively of 10 mm, 13 mm and 16 mm diameter. These Authors observed that a partial volume effect needs to be considered for axes ≤ 10 mm, whereas the larger ones were correctly estimated [6]. In our work we have instead considered phantoms of irregular shape, such that in some parts of them the thickness was less than 10 mm. This choice was made to evaluate the ability of our SPECT-CT acquisition system to estimate volumes different from a sphere or a rotation ellipsoid, since in clinical practice the target volume is not always comparable to symmetric geometric shapes. Moreover, we considered also as possible a thickness under one centimeter in relation to the shape of the phantoms used. In particular, phantoms of group B is one centimeter or even less thick for at least one third of its length.

As a last remark, the neck phantom used in our work does not allow the possibility of having a background activity. Therefore this method should not be used in clinical cases with poor contrast, although it is not frequently found.

For several decades, radioiodine treatment has been a well-established therapeutic choice in patients with hyperthyroidism due to its safety, effectiveness and low cost. Although the use of fixed doses for the treatment of hyperthyroidism, based on personal experience and literature data, is still common

in several Nuclear Medicine Departments, a dosimetry approach in accordance with the ALARA (As Low As Reasonably Achievable) philosophy is nevertheless desirable. The weight of the target mass is among the most important parameters for the outcome of therapy. Several methods have been proposed for the quantification of the mass of the thyroid gland or of the nodules to be given radiometabolic therapy with ^{131}I-iodide. They include CT, MR, US, planar scintigraphy, SPECT and PET. In particular, US is generally considered the method of choice for its suitability and cost-effectiveness, but it is based on the assumption that the thyroid nodule or lobes can be approximated by ellipsoids. The inherent uncertainty introduced by this method often exceeds 20 %, depending on the shape and size of the target volume. It has been observed that larger errors occur when the measured volume does not correspond to the metabolic active target tissue [18]. Some authors demonstrated the superiority of 3-D US volumetric calculations over 2-D US, especially when a manual tracking method is preferred to the ellipsoid model. These advantages were evident both for regularly shaped phantoms and deformed phantoms. Statistical analysis revealed that sensor navigation and mechanical sweeping techniques were equally suitable for 3-D US [19]. In order to optimize and simplify the diagnostic-therapeutic path, some authors have experienced many methods for measuring the thyroid volume avoiding the dependence on US or on other radiological methods. Ronga et al. successfully treated with a single dose of I131-iodide 93% of 1402 patients with solitary thyroid nodule hyperfunctioning [20], calculating the therapeutic dose through Marinelli formula as simplified by Haines and Keating [21]. The weight of each nodule was estimated palpatory. Besides the considerable experience required, this method of measurement can lead to an overestimation of small nodules and an underestimation of large nodules. In fact, these Authors reported a greater responsiveness of small nodules to treatment with respect to larger ones [20].

Different methods of estimating the target volume from the scintigrapy planar image have also been developed. Among the different formulas proposed, the following are worth mentioning: Brämstang's Method (Brämstang, 1968): V = area x 0.75 x b; Modified Brämstang's Method: V = area x c [5]; Lund's Method: V = π / 6 x a x b x c [5, 22], where the delimitation of the cross-sectional area is calculated using a fixed threshold of 10% of the maximum pixel, a and b are respectively the long and the short axis of the ellipse in the anterior planar image, c is the average thickness in a lateral scintigram. Moreover, a reasonable accuracy in volume quantification by SPECT has already been demonstrated. Van Isselt et al. found SPECT a valid alternative to US in the measurement of the thyroid volume in 25 patients with Graves' disease, employing a dual-detector SPECT camera with two gadolinium-153 transmission line sources. A fix threshold of 45% was used for the segmentation of the gland, as established in patient studies using a Minimal Mean Squared Error method (for

SPECT: $R^2 = 0.84$; bias = 1.8 ± 11.9 ml; for US: $R^2 = 0.97$; bias = 6.8 ± 7.5 ml). Planar scintigraphy correlated poorly with MRI ($R^2 = 0.61$) and suffered from a considerable bias (-4 ± 17.6 ml) [9].

The threshold should be adapted to each patient since it depends on various factors, as demonstrated by Mortelmans et al. (23). In fact, these Authors have verified the dependence on the contrast and on the size of the phantom. Volumes calculated in phantom studies were instead very similar with and without the attenuation compensation using a body contour obtained by acquisition of Compton and presuming a constant attenuation factor. With our study, we demonstrated also the dependence of the threshold on the shape of the phantom both in SPECT and in SPECT-CT measurements (**Figure 9**).

In this context, it is worth mentioning the adaptive threshold or gray level histogram method, based on SPECT imaging, able to establish the threshold that maximizes the separability of the object from the surround (Otsu, 1979). In clinical application the distinction between the class of organ pixels from that of background pixels is not always clear because the valley is not sufficiently deep or because there is a preponderance of one class without any valley [23]. In addition, the method is shown to fail for small volumes where the errors introduced by the partial volume effect are significant [5].

With our method, the calculation of the target volume is simple and quick to achieve. Furthermore, since it is based on an automatic contouring system, it is to be considered essentially operator-independent. As far as the study on phantoms is concerned, SPECT-CT showed a lower variability with respect to SPECT and, even lower with respect to the planar method. The subanalysis conducted for two different depths also showed lower SE and MAPE values for the SPECT-CT at the shallower depth. Furthermore, even though we enrolled only a small number of patients, our study revealed a lower percentage difference in volume estimation in most patients for SPECT-CT with respect to SPECT and planar methods compared to CT gold standard. It is interesting to note that the difference between the two tomographic methods is particularly evident in in the case of the ectopic basowified tissue (lesion “a”) and in the two cases in which the target volume was a partially retrosternal hot nodule (lesion “c” and lesion “d”), in addition to a case of Graves’ disease (lesion b). In only one case (lesion “e”), the estimated volume was very different from the gold standard for all three methods; this observation could be explained by a greater influence of the partial volume effect in the case of small lesions. Therefore, in cases in which the variable attenuation is influenced by tissues of different densities, a CT-based attenuation correction method could be particularly useful for measuring the target volume. However, the automatic contouring of the target volume with the software version that we used in the presence of a hyperfunctioning multinodular goiter cannot be applied for lesions with different radiotracer uptake. This can be explained by the fact that the system generates ROIs with a fixed threshold with respect to the point of maximum uptake in the whole series of images. Therefore,

an underestimation of the volume occurs in the case of less hyperfunctioning nodules. An underestimation in the measurements may also occur in those cases in which the accumulation of the radiotracer in the salivary glands is greater than in the thyroid nodule. In similar situations an acidic stimulus could be useful, such as the oral administration of lemon juice.

5. CONCLUSION

Thyroid tissue volumetry continues to be a challenge in pre-therapeutic evaluation of radioiodine treatment of hyperthyroidism. An accurate measurement of the target volume is of primary importance in theragnostics of benign thyroid disorders, both for the successful outcome of radioiodine treatment and for lower complication achievable for patients with a calculated dose strategy [24]. Our study confirms the superiority of SPECT in volume measurement if compared with the planar method. A more accurate measurement can be obtained from SPECT-CT, particularly when the tissue to be measured is very deep, as in the case of goiters or retrosternal nodules. In our opinion, the results shown here could encourage further studies in which more patients, affected by hyperthyroidism and candidates to radioiodine treatment, may be enrolled for a target volume estimation by means of a fix threshold-based volumetry method from 99mTc–pertechnetate SPECT-CT.

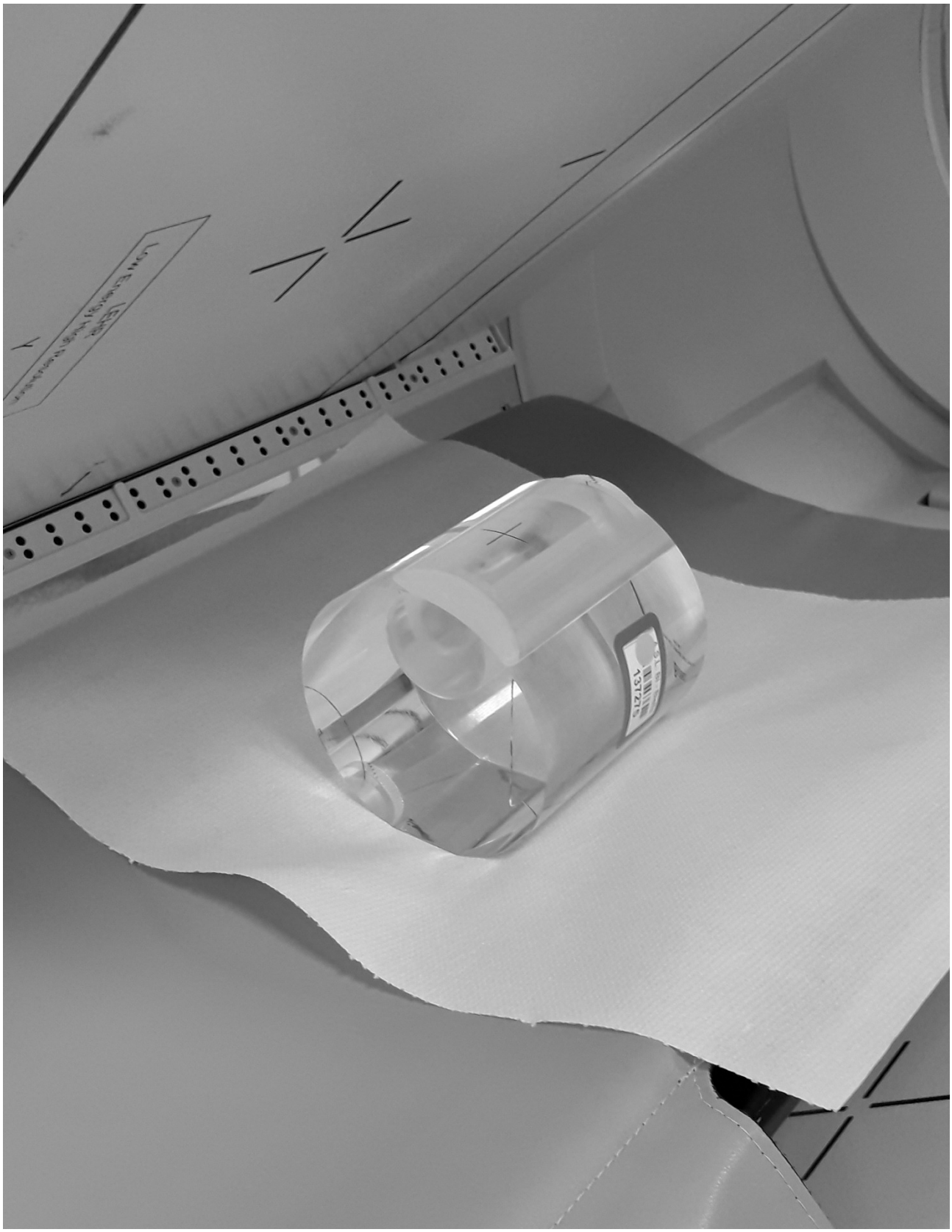

Figure 1

A photograph of the neck phantom we used, with a vial inside containing 15 ml of radioactive liquid.

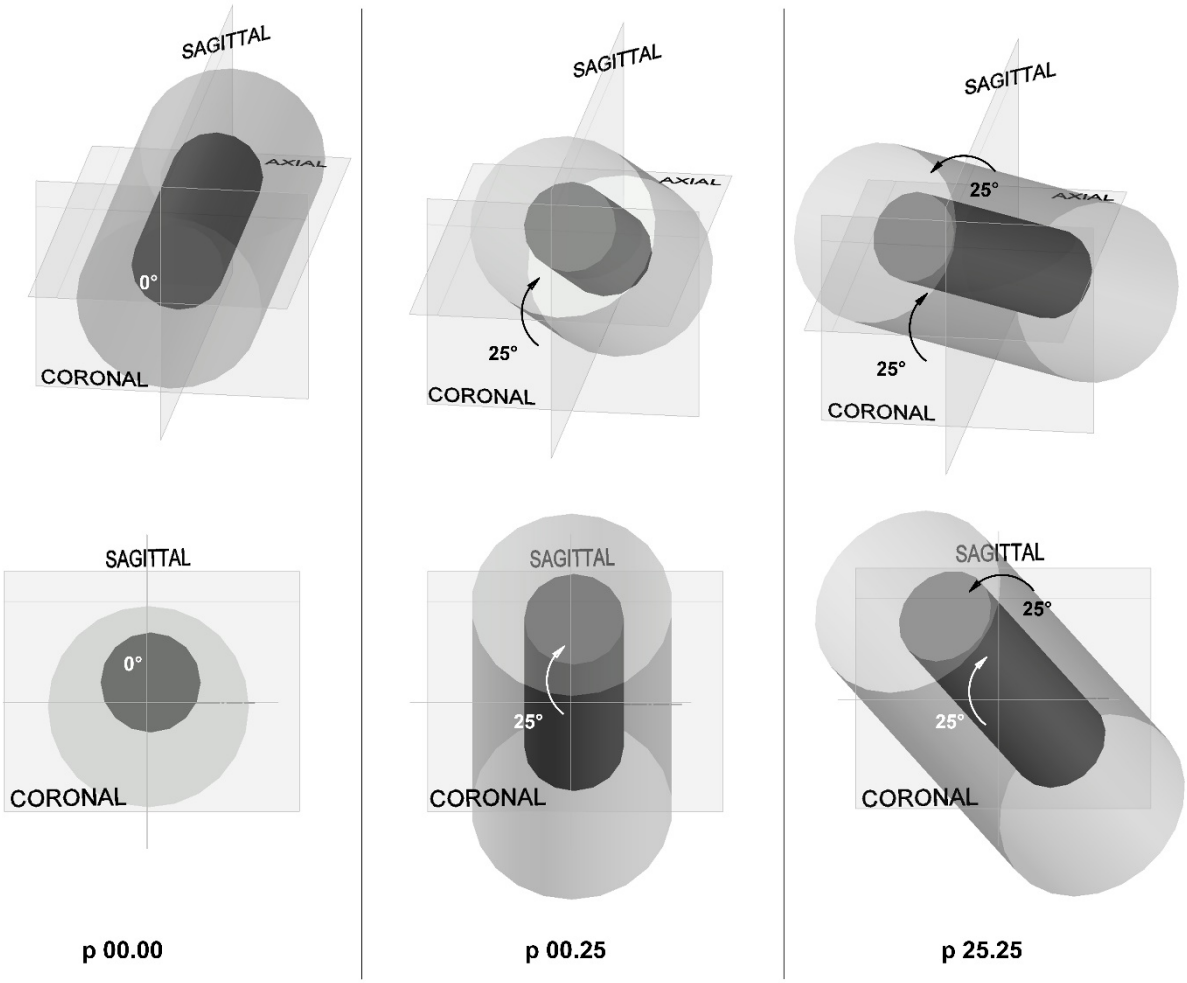

Figure 2

Examples of different orientations of the neck phantom in the space - p 00.00: the neck phantom, seplified in the figure as a cylinder, is in horizontal position along the axis of the bed; p 00.25: the phantom is tilted upwards by 25°; p 25.25: it is oriented by 25° both with respect to the coronal and sagittal plane.

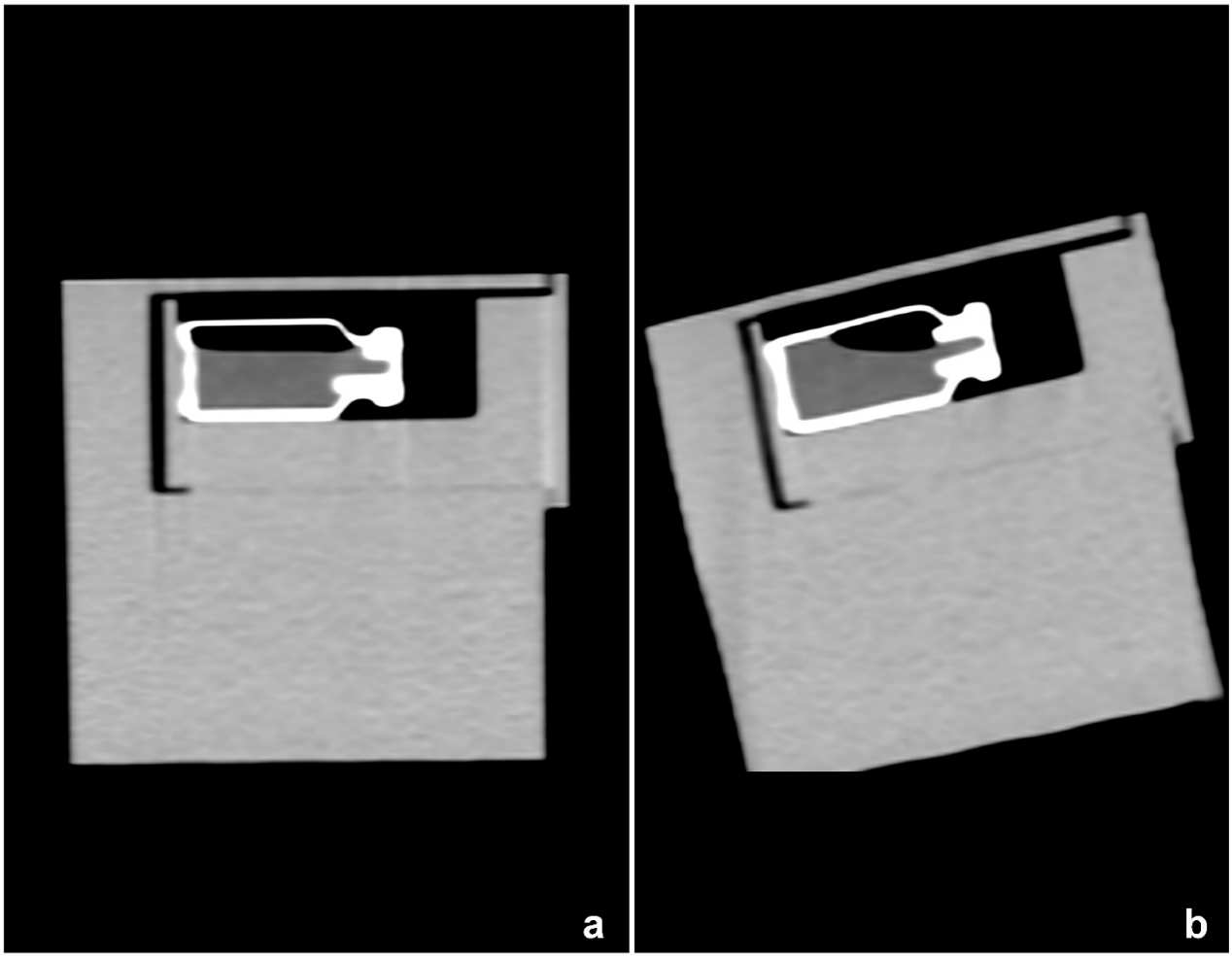

Figure 3

Two different orientations of the neck phantom in sagittal view, p00.00 and p 00.25, allow the radioactive liquid to obtain two different forms, respectively called A (a) and B (b).

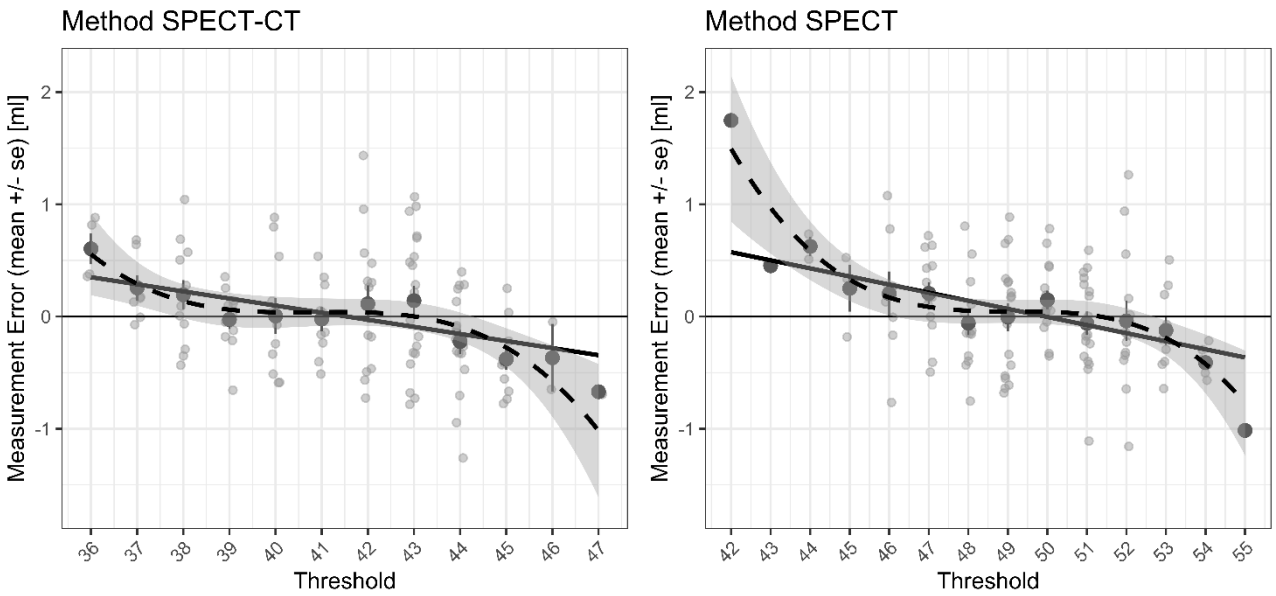

Figure 4

Linear and spline regression models for the volume estimation error as a function of the threshold values. Single measurement errors (shaded dots), error mean and standard deviations (gray bold dots with bars), linear model (continuous black line) and spline model (dashed black line) with prediction interval (shaded area) are plotted. Do notice x-scales are different in the two panels.

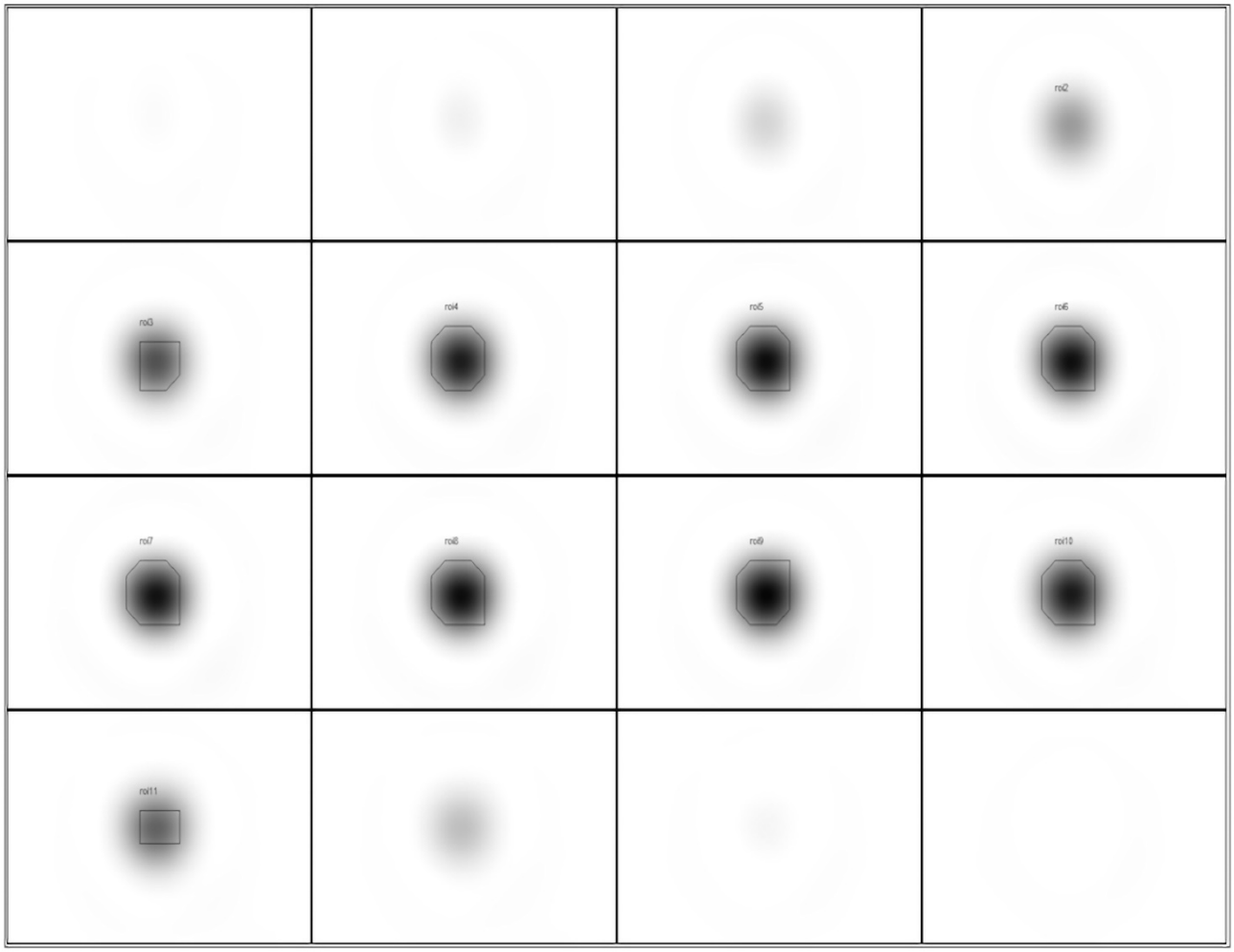

Figure 5

SPECT-CT axial cross-section with superimposed ROIs obtained automatically by means of a 41% threshold.

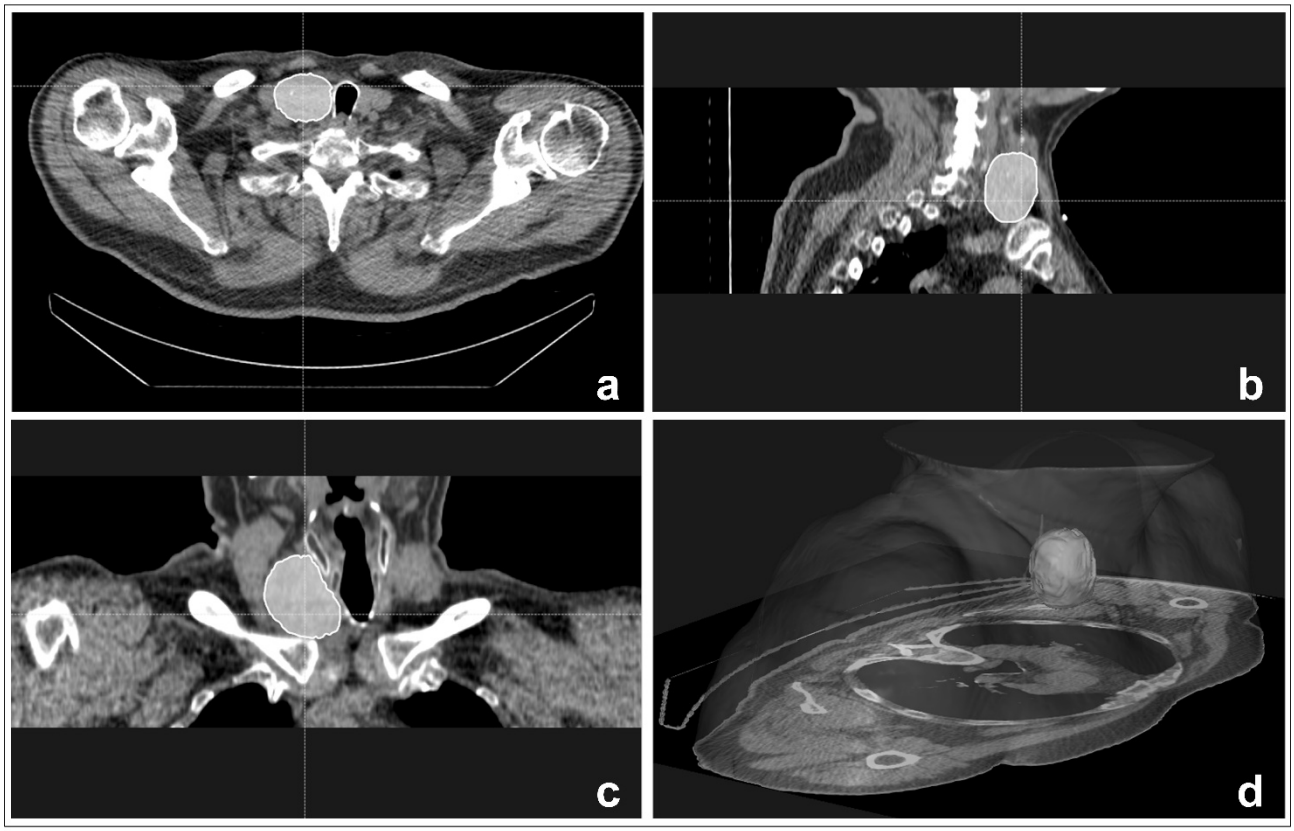

Figure 6

CT in axial, sagittal and coronal views with corresponding ROIs drawn manually around the nodule of the right thyroid lobe (a,b,c). 3-D rendering of the same lesion is also shown (d).

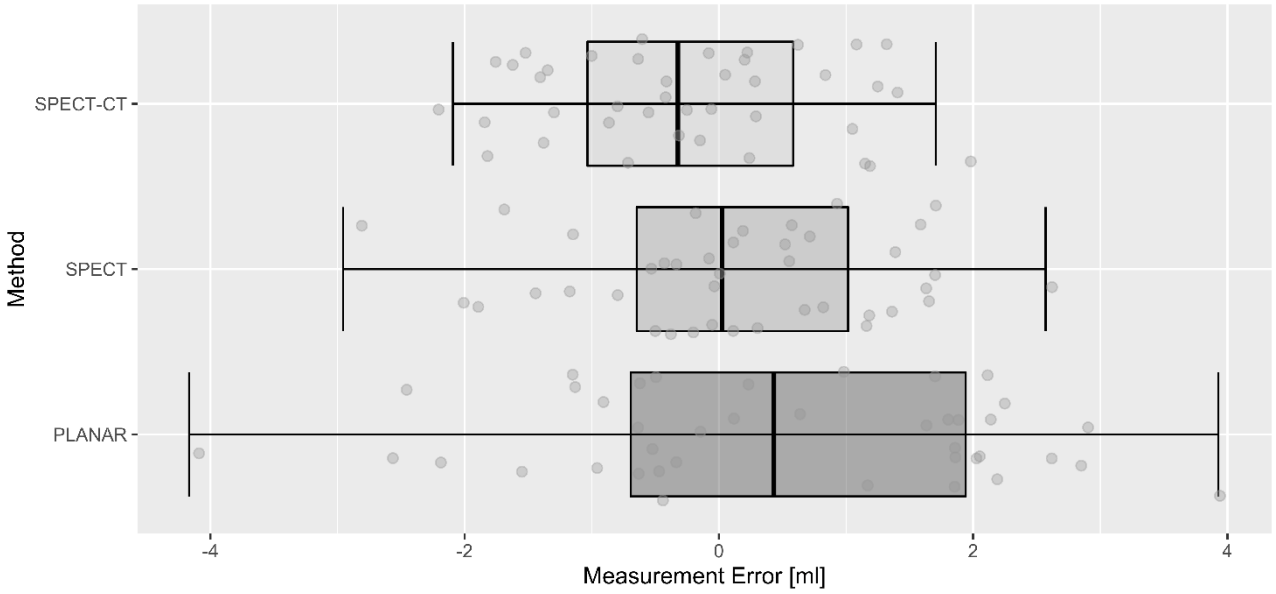

Figure 7

Boxplots of the measurement errors for the three methods: PLANAR, SPECT and SPECT-CT.

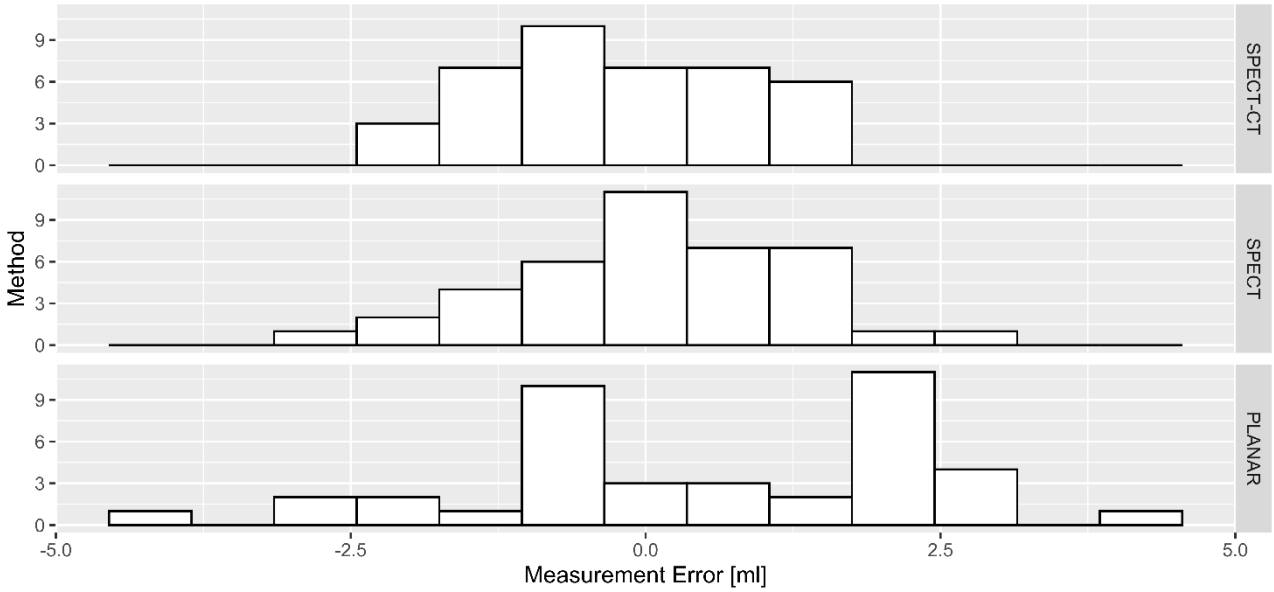

Figure 8

Histograms of the measurement errors for the three methods: PLANAR, SPECT and SPECT-CT.

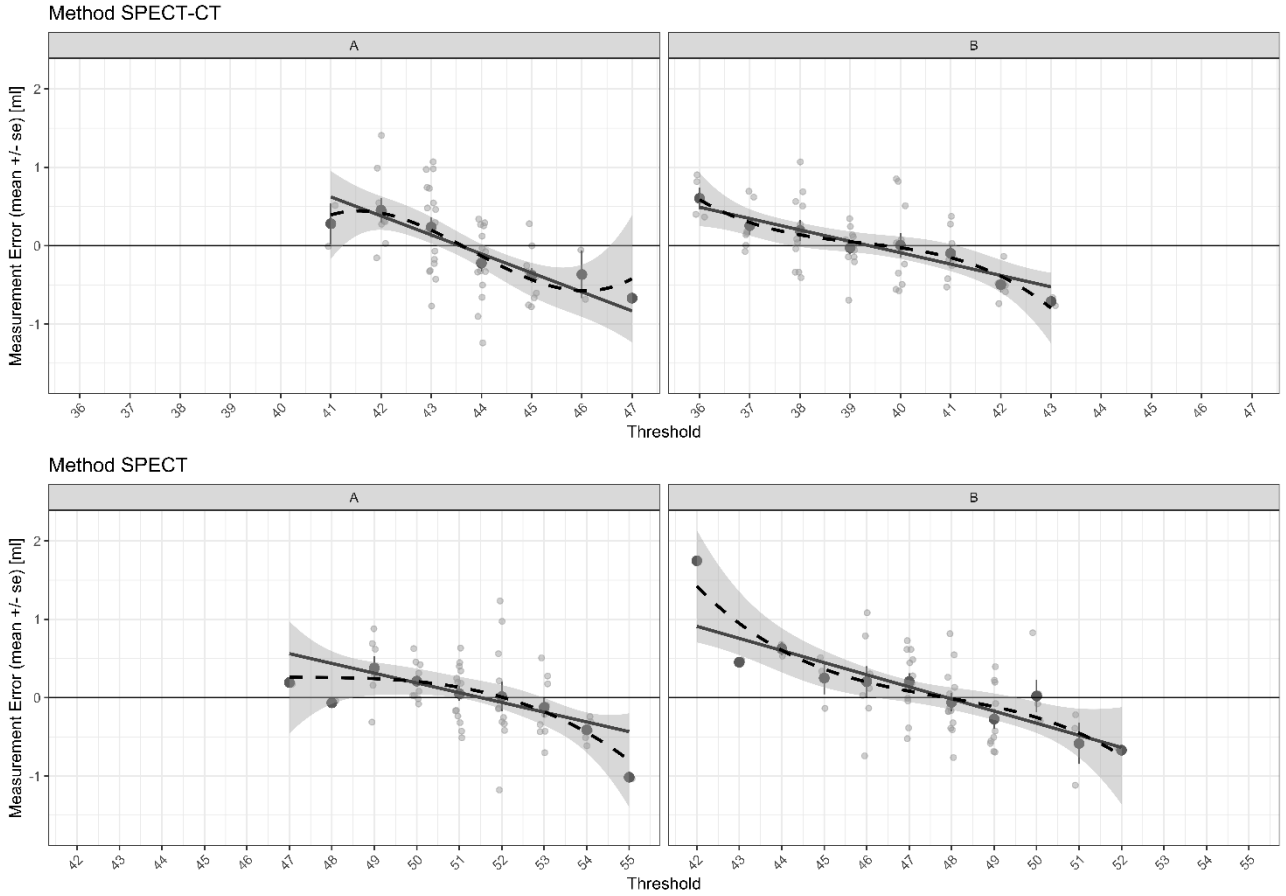

Figure 9

Linear and spline regression models for the dependency of the volume estimation error on the chosen threshold for the two different shapes of the radioactive liquid, A and B. It is well appreciated the dependence of the threshold on the shape of the phantom both in SPECT and in SPECT-CT measurements.

LIST OF ABBREVIATIONS

Ultrasound = US

Computed Tomography = CT

Magnetic Resonance = MR

Single Photon Emission Computed Tomography – Computed Tomography = SPECT-CT

Single Photon Emission Computed Tomography = SPECT

Standard Deviation = SD

Standard Error = SE

Mean Absolute Percentage Error = MAPE

Root Mean-Square Error = RMSE

99mTc-pertechnetate = $^{99m}TcO_4^-$

Thyroid Uptake of $^{99m}TcO_4^-$ = TCTU

ETHICAL APPROVAL AND CONSENT TO PARTICIPATE

All human procedures were followed in accordance with the ethical standards of the committee responsible for human experimentation (institutional and national).

HUMAN AND ANIMAL RIGHTS

No animals were used in this research. The reported experiments were performed in accordance with the ethical standards of the committee responsible for human experimentation (institutional and national), and with the Helsinki Declaration of 1975, as revised in 2013 (http://ethics.iit.edu/ecodes/node/3931).

CONSENT FOR PUBLICATION

Informed consent was obtained from all individual participants included in the study.

AVAILABILITY OF DATA AND MATERIALS

The datasets used during the current study are available from the corresponding author on a reasonable request.

FUNDING

None.

CONFLICT OF INTEREST

The authors confirm that this article content has no conflict of interest.

ACKNOLEDGEMENTS

Dr. Roberta Maoret and Dr. Leonardo Jon Scotta of Fondazione 3Bi – Biblioteca Biomedica Biellese are gratefully acknowledged for the assistance in bibliographic research.

BIBLIOGRAPHY

1) Germano, A.; Schmitt, W.; Carvalho, M.R.; Marques, R.M. Normal Ultrasound Anatomy and Common Anatomical Variants of the Thyroid Gland Plus Adjacent Structures - A Pictorial Review. *Clin Imaging,* **2019**, 58:114-128.

2) Lee, H.J.; Yoon, D.Y.; Seo, Y.L.; Kim, J.H.; Baek, S.; Lim, K.J.; Cho, Y.K.; Yun, E.J. Intraobserver and Interobserver Variability in Ultrasound Measurements of Thyroid Nodules**.** *J Ultrasound Med,* **2018,** 37(1):173-178.

3) Lyshchik, A.; Drozd, V.; Reiners, C. Accuracy of Three-Dimensional Ultrasound for Thyroid Volume Measurement in Children and Adolescents, *Thyroid,* **2004**, 14(2):113-120.

4) Hanson, M.A.; Shaha, A.R.; Wu, J.X. Surgical approach to the substernal goiter, *Best Pract Res Clin Endocrinol Metab,* **2019,** 33(4):101312.

5) Zaidi, H. Comparative Methods for Quantifying Thyroid Volume Using Planar Imaging and SPECT, *J Nucl Med*, **1996,** 37(8):1421-1426.

6) Matheoud, R.; Canzi, C.; Reschini, E.; Zito, F.; Voltini, F.; Gerundini, P. Tissue-specific Dosimetry for Radioiodine Therapy of the Autonomous Thyroid Nodule. *Med Phys*, **2003,** 30(5):791-798.

7) Calandri, E.; Filippi, L.; Aretano, I.; Pultrone, M. *Indian J Nucl Med,* **2021,** 36(1): 97-99.

8) Pant, G.S.; Kumar, R.; Gupta, A.K.; Sharma, S.K.; Pandey, A.K. Estimation of Thyroid Mass in Graves' Disease by a Scintigraphic Method. *Nucl Med Commun*, **2003,** 24(7):743-748.

9) van Isselt, J.W.; de Klerk, J.M.; van Rijk, P.P.; van Gils, A.P.; Polman, L.J.; Kamphuis, C.; Meijer, R.; Beekman, F.J. Comparison of Methods for Thyroid Volume Estimation in Patients With Graves' Disease. *Eur J Nucl Med Mol Imaging,* **2003,** 30(4):525-531.

10) Frangos, S.; Buscombe, J.R. Why should we be concerned about a "g"? *Eur J Nucl Med Mol Imaging,* **2019,** 46(2):519.

11) Dottorini, M.E.; Inglese, E.; Salvatori, M.; Signore, A.; Squatrito, S.; Vitti, P. Linee Guida SIE-AIMN-AIFM per il Trattamento Radiometabolico dell'Ipertiroidismo. Vrs aggiornata 02/2005. Available from: https://www.aimn.it › pubblicazioni › LG_ipertiroidismo_05 (last access May 20, **2021**).

12) Hastie, T.; Tibshirani, R.; Friedman, J. *The Elements of Statistical Learning: Data Mining, Inference, and Prediction,* 2nd ed.; Springer Nature, **2013**.

13) Meller, J,; Becker, W. Scintigraphy with 99mTc-pertechnetate in the evaluation of functional thyroidal autonomy. *Q J Nucl Med,* **1999**, 43(3):179-187.

14) Meller, J.; Becker, W. The continuing importance of thyroid scintigraphy in the era of high-resolution ultrasound. *Eur J Nucl Med Mol Imaging,* **2002,** 29 Suppl 2:S425-438.

15) Rumack, C.M.; Levine, D. *Diagnostic ultrasound,* 5th ed.; Elsevier: Philadelphia, **2018**.

16) Nataf. A. *Chiffres-repères-mesures-classifications en imagerie médicale*; Sauramps medical: Montpellier, **2014**.

17) Riccabona, M. *Pediatric Ultrasound Requisites and Applications*, 2nd ed.; Springer: London, **2014**.

18) Hänscheid, H.; Canzi, C.; Eschner, W.; Flux, G.; Luster, M.; Strigari, L.; Lassmann, M. EANM Dosimetry Committee Series on Standard Operational Procedures for Pre-Therapeutic Dosimetry II. Dosimetry Prior to Radioiodine Therapy of Benign Thyroid Diseases. *Eur J Nucl Med Mol Imaging*, **2013**, 40(7):1126-1134.

19) Freesmeyer, M.; Wiegand, S.; Schierz, J.H.; Winkens, T.; Licht, K. Multimodal Evaluation of 2-D and 3-D Ultrasound, Computed Tomography and Magnetic Resonance Imaging in Measurements of the Thyroid Volume Using Universally Applicable Cross-Sectional Imaging Software: A Phantom Study. *Ultrasound Med Biol,* **2014,** 40(7):1453-1462.

20) Ronga, G.; Filesi, M.; D'Apollo, R.; Toteda, M.; Di Nicola, A.D.; Colandrea, M.; Travascio, L.; Vestri, A.R.; Montesano, T. Autonomous Functioning Thyroid Nodules and 131I in Diagnosis and Therapy After 50 Years of Experience: What Is Still Open to Debate? *Clin Nucl Med*, **2013**, 38(5):349-353.

21) Marinelli, L.D.; Quimby, E.H.; Hine, G.J. Dosage Determination With Radioactive Isotopes; Practical Considerations in Therapy and Protection. *Am J Roentgenol Radium Ther,* **1948**, 59(2):260-281.

22) Olsen, K.J. Scintigraphic Estimation of Thyroid Volume and Dose Distribution at Treatment With 131I. *Acta Radiol Oncol Radiat Phys Biol*, **1978**, 17(1):74-80.

23) Mortelmans, L.; Nuyts, J.; Van Pamel, G.; Van den Maegdenbergh, V.; De Roo, M.; Suetens, P. A new thresholding method for volume determination by SPECT. *Eur J Nucl Med,* **1986**;12(5-6):284-290.

24) Ariamanesh, S.; Ayati, N.; Mazloum Khorasani, Z.; Mousavi, Z.; Kiavash V.; Kiamanesh, Z.; Zakavi, S.R. Effect of Different 131I Dose Strategies for Treatment of Hyperthyroidism on Graves' Ophthalmopathy. *Clin Nucl Med,* **2020,** 45(7):514-518.